



# ZIP14 is degraded in response to manganese exposure

Khristy J. Thompson  · Marianne Wessling-Resnick

Received: 20 May 2019 / Accepted: 10 September 2019 / Published online: 20 September 2019  
© The Author(s) 2019

**Abstract** Manganese (Mn) is an essential element necessary for proper development and brain function. Circulating Mn levels are regulated by hepatobiliary clearance to limit toxic levels and prevent tissue deposition. To characterize mechanisms involved in hepatocyte Mn uptake, polarized human HepaRG cells were used for this study. Western blot analysis and immunofluorescence microscopy showed the Mn transporter ZIP14 was expressed and localized to the basolateral surface of polarized HepaRG cells. HepaRG cells took up  $^{54}\text{Mn}$  in a time- and temperature-dependent manner but uptake was reduced after exposure to Mn. This loss in transport activity was associated with decreased ZIP14 protein levels in response to Mn exposure. Mn-induced degradation of ZIP14 was blocked by bafilomycin A1, which increased localization of the transporter in Lamp1-positive vesicles. Mn exposure also down-regulated the Golgi proteins TMEM165 and GPP130 while the ER stress marker BiP was induced. These results indicate that Mn exposure decreases ZIP14 protein levels to limit subsequent uptake of Mn as a cytoprotective response. Thus, high levels of Mn may compromise first-pass-hepatic clearance mechanisms.

**Keywords** SLC39A14 · Hepatocytes · HepaRG cells · Mn homeostasis

## Introduction

Manganese is required for a number of essential physiological processes such as bone development, immunity, brain function, and overall homeostasis (Aschner and Aschner 2005; Aschner and Erikson 2017; Roth 2006). As is the case with many essential nutrients, there is a fine balance between adequate levels of Mn and harmful concentrations. It has long been established that excess Mn results in functionally diminished motor pathways, impaired cognition, and attention disorders (Aschner and Erikson 2017; Crinella 2012; Hong et al. 1984; Lucchini et al. 1997; Pihl and Parkes 1977; Tran et al. 2002; Yamada et al. 1986). To protect the body against excessive harmful levels, ingested Mn is trafficked to the bile through the first-pass hepatic clearance. This protective mechanism is thought to limit excess circulating Mn to protect the body from its neurotoxic effects. An increasing number of animal studies and human genetic studies provide strong evidence that ZIP14 (SLC39A14) is a primary regulator of balanced blood Mn levels. Individuals carrying mutations ZIP14 display hypermanganesemia (Clayton 2017). Defects in ZIP14 cause high blood Mn with Mn loading in the

---

K. J. Thompson (✉) · M. Wessling-Resnick  
Department of Genetics and Complex Diseases, Harvard  
T.H. Chan School of Public Health, 665 Huntington  
Avenue, Boston, MA 02115, USA  
e-mail: kthompso@hsph.harvard.edu

brain but not in liver, indicating that its function in liver uptake must be impaired (Tuschl et al. 2016). Several human mutations in ZIP14 have been identified in young children suffering from parkinsonism-dystonia with high blood Mn levels (Juneja et al. 2018; Rodan et al. 2018) as well increased cerebral spinal fluid Mn (Marti-Sanchez et al. 2018).

While the combined data from human and animal studies have identified ZIP14 as an essential component of Mn regulation and homeostasis, it is clear that tissue specific mechanisms of transport regulation are just beginning to be elucidated. In previous studies of polarized WIF-B cells, we determined that hepatobiliary trafficking of Mn involved multiple transporters. The transporters were localized to precise cellular locations to mediate vectorial delivery of Mn from the sinusoidal basolateral surface to the bile canalicular apical membrane of hepatocytes (Thompson et al. 2018). ZIP14 localization at the basolateral surface of these hepatic cells is consistent with a role in Mn import (Aydemir et al. 2017; Hutchens et al. 2017; Jenkitkasemwong et al. 2018). In contrast, the Mn transporter ZIP8 (SLC39A8) was found to distribute to cytoplasmic vesicular structures while ZNT10 (SLC30A10) was present in vesicles adjacent to the WIF-B cell apical membrane. A limitation to these studies was the fact that both rat and human ZIP14 transporters were expressed in this rat-human hybrid line. Therefore, to further our understanding of the role of ZIP14 in hepatocyte Mn uptake and clearance, we have now studied its function in polarized HepaRG cells which are a human-derived hepatocytoma line. HepaRG cells have been used extensively in drug clearance and toxicity studies. These cells express a large array of the liver specific genes at greater quantities than other hepatocyte cells lines, as well as both sinusoidal and canalicular drug transporters (Aninat et al. 2006; Le Vee et al. 2006; Pernelle et al. 2011). The present study is the first analysis of Mn transport and metabolism in these human hepatic cells. Our goals were to evaluate Mn accumulation by HepaRG cells and to explore mechanisms regulating Mn import under conditions of hypermanganesemia.

## Methods

### Cell culture

For uptake and ICP-MS experiments, HepaRG cells (MTOX1010; Millipore Sigma) were seeded into 24-well plates in Williams' medium (Gibco) supplemented with HepaRG Thaw General Purpose Supplement (Life Technologies) and 1X GlutaMAX Supplement (Life Technologies) according to supplier guidelines. For immunofluorescence microscopy experiments, HepaRG cells were seeded on transwell inserts (0.4 micron PET; Corning Falcon Cell Culture Inserts) which require fewer cells (cell growth area approximately half the area of the 24-well). Similar morphology and Zip14 distribution were observed in cells plated on coverslips. To ensure polarization, cells were maintained in culture for 10–12 days with 5% CO<sub>2</sub> at 37 °C. All treatment conditions and uptake studies were performed at a volume of 300 µL per well. Washes between conditions and terminal washes were performed at a volume of 1000 µL as detailed in the following procedures.

### Temperature and time-dependent Mn uptake

Uptake dynamics were established through <sup>54</sup>Mn tracer uptake studies. <sup>54</sup>Mn was purchased from PerkinElmer (NEZ040) and specific activity was adjusted to 145 cpm/pmol with cold MnCl<sub>2</sub>. HepaRG cells were incubated in uptake buffer containing standard 1 × Hanks Balance Salt Solution (HBSS; Gibco) with 1 µM <sup>54</sup>MnCl<sub>2</sub> at 37 °C or on ice (4 °C) for 5, 10, 30, or 60 min. Cells were rinsed in ice-cold Ca<sup>2+</sup>/Mg<sup>2+</sup> free HBSS + 100 µM EGTA 3 times at the end of incubation to remove any extracellular non-specifically bound metal and release Mn targeted to the bile compartment which is sensitive to calcium chelation (Suda et al. 2011). Uptake was limited to shorter uptake incubation times since by 4 h, cells were not viable in serum-free HBSS uptake medium. At the end of the uptake incubation period and after EGTA washes, cells were immediately lysed in Laemmli buffer, removed from the plate, and the radioactivity of each sample was measured in a WIZARD Gamma Counter (PerkinElmer, Inc., Waltham, MA, USA). Cell uptake was calculated as pmol/well. Cell-associated radioactivity measured at 4 °C was taken as non-specific background.

## Competition studies

To test if excess metal could compete for  $^{54}\text{Mn}$  uptake, HepaRG cells were incubated in uptake buffer containing  $1\ \mu\text{M}$   $^{54}\text{MnCl}_2$  with an additional 5 or  $50\ \mu\text{M}$   $\text{MnCl}_2$  for 30 min at  $37\ ^\circ\text{C}$ . Cells were rinsed three times in cold HBSS containing  $100\ \mu\text{M}$  EGTA. Cells were lysed in Laemmli buffer, removed from the plate, and the radioactivity of each sample was measured in a WIZARD Gamma Counter (PerkinElmer, Inc., Waltham, MA, USA).

## Effects of Mn exposure on Mn uptake

HepaRG cells were exposed to indicated concentrations of  $\text{MnCl}_2$  in standard culture media for 4 or 16 h prior to uptake studies. The standard culture media contained  $1.8\ \text{mM}$   $\text{CaCl}_2$  and provided a source for competition of non-specific divalent metal binding sites. Media containing added metal was removed and cells were rinsed with standard HBSS followed by incubation for 30 min at  $37\ ^\circ\text{C}$  in uptake buffer containing  $1\ \mu\text{M}$   $\text{MnCl}_2$ . After uptake, the cells were placed on ice and washed 3 times with  $1\ \text{mL}$  cold  $\text{Ca}^{2+}/\text{Mg}^{2+}$  free HBSS containing  $100\ \mu\text{M}$  EGTA. Cells were then lysed in  $1 \times$  Laemmli buffer and radioactivity was measured. Samples were subsequently analyzed for transporter levels by Western blot analysis. In a separate set of experiments Mn content was measured using ICP-MS (inductively coupled mass spectrometry) carried out by Dartmouth Trace Element Shared Resource. HepaRG cells exposed to Mn were washed with cold PBS, trypsinized to remove nonspecifically bound extracellular Mn, and cell pellets collected and weights recorded. ICP-MS analysis was performed by the Trace Metals Analysis Laboratory (Dartmouth College, Hanover, NH) and Mn content was normalized to the cell pellet wet weights.

## Bafilomycin A1 treatment

To test if the decrease in ZIP14 protein levels following Mn treatment was due to lysosomal degradation, HepaRG cells were treated with  $50\ \text{nM}$  bafilomycin A1 for 30 min prior to the addition of Mn.  $50\ \text{nM}$  bafilomycin A1 was subsequently maintained in the medium upon the addition of  $50\ \mu\text{M}$  Mn for 4 h in standard culture conditions. Control wells

were incubated with or without  $50\ \mu\text{M}$  Mn in the absence of bafilomycin A1. At the end of the experiment, cells were rinsed with warm HBSS, lysed in Laemmli buffer and processed for Western blot analysis.

## Western blot analysis

HepaRG cells were exposed to indicated concentrations of  $\text{MnCl}_2$  for 4 or 16 h in standard culture conditions. Following treatment, the cells were rinsed in  $1\ \text{mL}$  standard culture media followed by two washes in PBS. Cells were lysed in  $1 \times$  Laemmli buffer and processed for Western blot analysis. HepaRG cells in  $1 \times$  Laemmli sample buffer containing beta-mercaptoethanol were heated for 5 min at  $95\ ^\circ\text{C}$  to blot for ZIP14, GPP130, and BiP, or 10 min at  $72\ ^\circ\text{C}$  to blot for TMEM165, GM130, ZNT10, and ferroportin (FPN). Samples for ZIP8 were unheated. Equivalent sample volumes were loaded onto 4–20% denaturing gels, proteins were separated by SDS-PAGE, and transferred to nitrocellulose (Bio-Rad Transblot Turbo blotting system). Immunoblots were blocked with 5% non-fat milk in Tris-buffered saline (TBS) containing 1% Tween-20 (TW20). Blots were then incubated with primary antibodies (rabbit anti-ZIP14, Sigma 1:1000; rabbit anti-ZIP8, Sigma 1:1000; rabbit anti-ZNT10, Sigma 1:1000; rabbit anti-FPN, Novus, 1:1000; rabbit anti-GPP130, BioLegend 1:500; rabbit anti-BiP, Cell Signaling Technologies 1:1000; rabbit anti-TMEM165, Sigma 1:1000; rabbit anti-GM130, Cell Signaling Technology 1:1000) in TBS-TW20 overnight at  $4\ ^\circ\text{C}$ . After two washes in TBS-TW20, blots were placed in secondary IRDye 800CW donkey anti-rabbit or anti-mouse IgG (Li-Cor, 1:5000 dilution) or IRDye 680RD donkey anti-rabbit or anti-mouse IgG (Li-Cor, 1:5000 dilution) and then rinsed in TBS-TW20. Glyceraldehyde 3-phosphate dehydrogenase (GAPDH) was as a loading control and detected using mouse anti-GAPDH (Sigma, 1:2000) or rabbit anti-GAPDH (ABclonal, 1:1000). Images were acquired on Li-COR Odyssey Clx Near-Infrared Western Blot System and band intensity analyzed using iS Image Studio.

## Indirect immunofluorescence of HepaRG cells

HepaRG cells were rinsed in phosphate-buffered saline (PBS), fixed in 4% paraformaldehyde in PBS

for 20 min, and quenched with 10 mM glycine in PBS. Cells were permeabilized for 5 min in 0.2% Triton-X100/PBS, followed by a 30-min blocking step with 1% bovine serum albumin (BSA) in PBS. Cells were then incubated for overnight at 4 °C with the following primary antibodies: rabbit anti-ZIP14 (Sigma 1:200), mouse anti-MRP2 (Abcam, 1:200), mouse anti-Lamp1 (Abcam, 1:100), mouse anti-beta1 NaK-ATPase (Abcam, 1:200, followed by a 45 min incubation with secondary antibodies AlexaFluor568-labeled goat anti-rabbit (Molecular Probes, 1:500), AlexaFluor568-labeled goat anti-mouse (Molecular Probes, 1:500), AlexaFluor488-labeled goat anti-rabbit (Invitrogen, 1:500), or AlexaFluor488-labeled goat anti-mouse (Invitrogen, 1:500). Inserts were mounted using ProLong Diamond Antifade Mountant (Invitrogen). Prior to fixation, nuclei were stained with NucBlue Live Cell Stain ReadyProbes according to manufacturer's instructions (Invitrogen). HepaRG cells were imaged with a Yokogawa CSU-X1 spinning disk confocal system with a Nikon Ti-E inverted microscope using a 60 × or 100 × Plan Apo objective lens with Zyla CMOS camera using 405, 561 and 488 lasers. NIS elements software was utilized for acquisition parameters, shutters, filter positions and focus control.

### Cell viability

Cell viability was determined using the TOX-1 assay (Sigma). Cells were first exposed to MnCl<sub>2</sub> (0, 5, 25, 50, 500, and 1000 μM) for 4 or 16 h, followed by a 4 h incubation with (3-[4,5-dimethylthiazol-2-yl]-2,5-diphenyl tetrazolium bromide) (MTT; 0.5 mg/mL). The formazan crystals produced in the reactions were then dissolved in isopropyl alcohol containing 0.1 N HCl. Absorbance of the samples was measured at 570 nm using a BioTek Synergy 2 plate reader. Cell viability was normalized to control (untreated) cells as recommended by the manufacturer.

### Statistical analysis

Statistical comparisons were performed using one-way ANOVA and Student's *t* test with GraphPad Prism software. Results are expressed as mean ± SEM. Differences between compared groups were considered significant at *P* < 0.05. Regression analysis were used to determine dose–response relationship

between transporter levels and manganese exposure. ImageJ software and the JACoP plugin were used to determine Pearson's coefficient where results are expressed as mean ± SD.

## Results

### HepaRG cells express ZIP14 and the transporter localizes to the basolateral surface

HepaRG cells polarize to mature hepatocytes and form confluent monolayers with bile canalicular formations. They have been utilized to study various transport mechanisms and have successfully been imaged using indirect immunofluorescence (Antherieu et al. 2013; Bachour-El Azzi et al. 2015; Kanebratt and Andersson 2008; Sharaneek et al. 2014; Susukida et al. 2016). To determine the expression and membrane distribution of ZIP14, we performed indirect immunofluorescence experiments co-labeling apical or basolateral markers. ZIP14 did not colocalize with the apical membrane marker MRP2 (Fig. 1a, left panel) but was exclusively localized to the basolateral surface with extensive overlap with the basolateral membrane marker NaK-ATPase (Fig. 1a, right panel). Placement of ZIP14 at the basolateral membrane is consistent with its function as a hepatocyte metal importer (Bowers and Srail 2018; Guthrie et al. 2015; Pinilla-Tenas et al. 2011; Zhao et al. 2014).

### Temperature and time dependent uptake of Mn by HepaRG cells

To determine the time course of Mn uptake by HepaRG cells, cellular acquisition of the radioactive tracer <sup>54</sup>Mn was measured. HepaRG cell Mn uptake occurred in a time- and temperature-dependent manner (Fig. 1b, c). The cellular uptake of <sup>54</sup>Mn was competed by excess unlabeled Mn (Fig. 1c). These observations support the specificity of the metal uptake pathway.

### HepaRG cells are resistant to Mn-induced cytotoxicity

Mn has been shown to be toxic to a variety of cell types at μM concentrations (Choi et al. 2019; Fernandes et al. 2019; Porte Alcon et al. 2018; Roth et al. 2002).

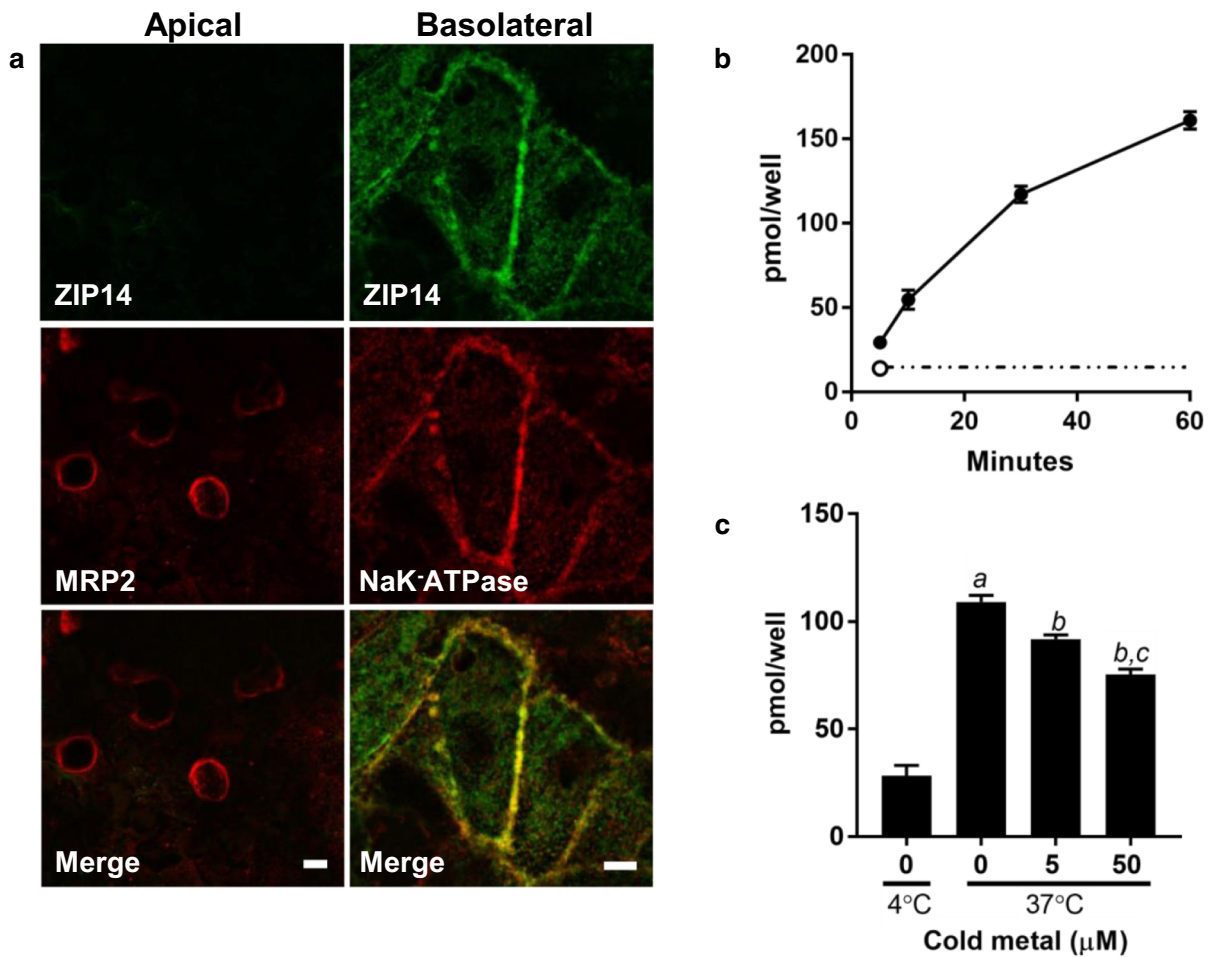


**Fig. 1** ZIP14 localization and Mn uptake by HepaRG cells. **a** ZIP14 colocalizes with the basolateral membrane marker NaK-ATPase but not the apical marker MRP2. HepaRG cells were grown on 0.4 μm transparent inserts for 12 days in standard culture conditions. Shown are staining for ZIP14 (green) and the apical marker MRP2 (left panel; red) or the basolateral marker NaK-ATPase (right panel; red) using indirect immunofluorescence. Cells were imaged using a Yokogawa CSU-X1 spinning disk confocal system with a Nikon Ti-E inverted microscope using a 60 × (MRP2 images) or a 100 × (NaK-ATPase images) Plan Apo objective lens with Zyla cMOS camera using 561 and 488 lasers. Bar = 5 μm. **b** Mn uptake is time and temperature dependent. HepaRG cells were incubated with 1 μM <sup>54</sup>Mn for 5, 10, 30 and 60 min at 37 °C

(filled circles). Uptake at 4 °C is indicated at 5 min (open circle) and extrapolated out to 60 min as indicated by the dashed line. After incubation for the times indicated, cells were washed, removed from the plate, and cell-associated <sup>54</sup>Mn was measured by gamma counting. Values are mean ± SEM, n = 4 biological samples. **c** <sup>54</sup>Mn uptake is competed by excess unlabeled Mn. Cells were incubated with 1 μM <sup>54</sup>Mn in uptake buffer containing either 5 or 50 μM cold Mn. After incubation for the times indicated, cells were washed, removed from the plate, and cell-associated <sup>54</sup>Mn was measured by gamma counting. Values are mean ± SEM, n = 4 biological samples; *a* significant from 4 °C; *b* significant from control; *c* significant from 5 μM Mn. *P* < 0.05

For example, in our previous studies WIF-B cells were observed to have significantly reduced viability after 4 and 16 h of exposure to > 500 μM Mn (Thompson et al. 2018). Therefore, we examined the viability of HepaRG cells after exposure of up to 1000 μM Mn for

4 or 16 h in standard culture conditions. Cell viability was determined using the MTT assay (Fig. 2a). HepaRG cells maintained close to 100% viability over all Mn concentrations at both exposure times. ICP-MS experiments confirmed that Mn did

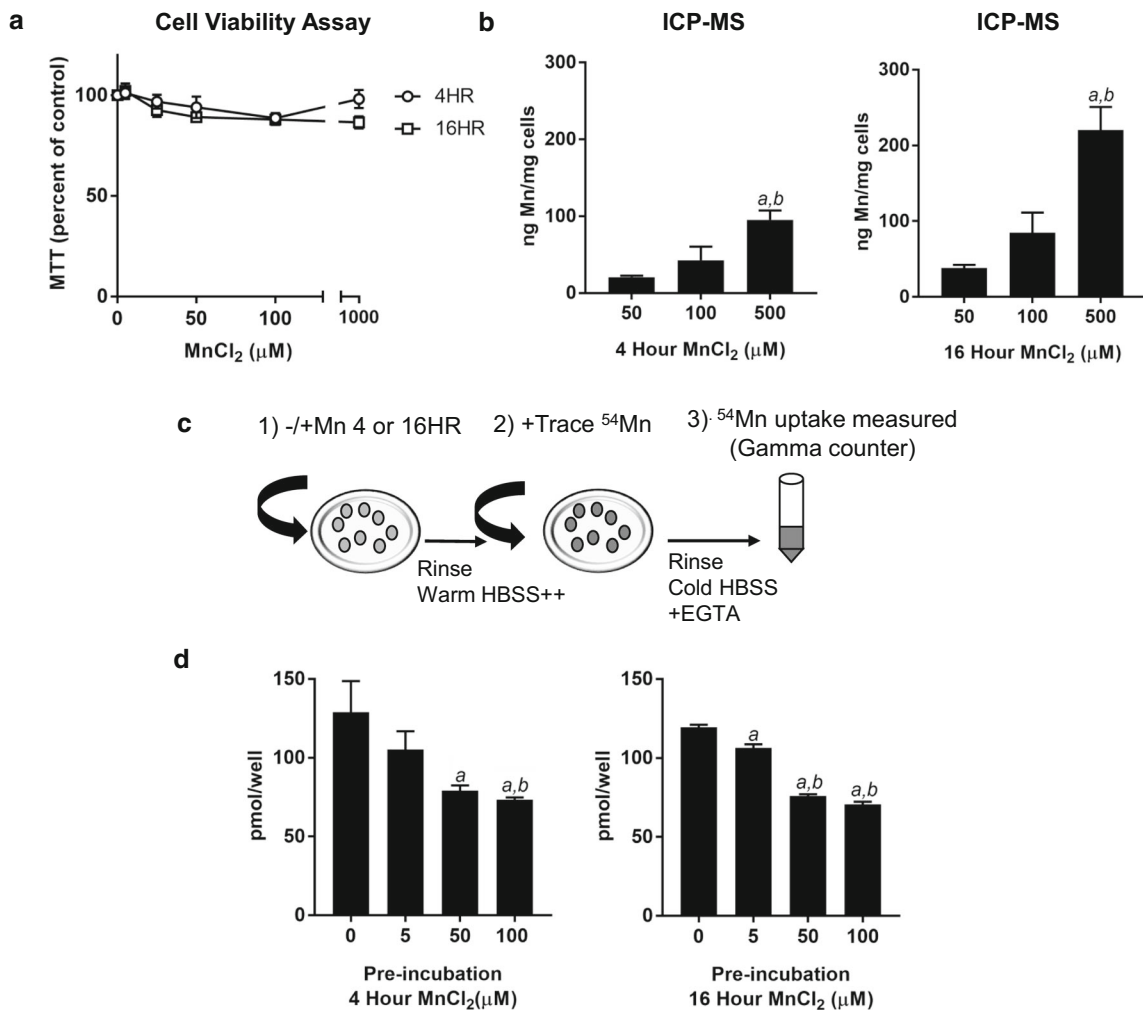


**Fig. 2** HepaRG cell response to 4 and 16 h Mn exposure. HepaRG cells were exposed to Mn for 4 and 16 h in standard culture conditions followed by assessment of cell viability or <sup>54</sup>Mn uptake. **a** HepaRG cells remain viable following exposure to Mn (5, 25, 50, 100, 1000 μM) for 4 h (open circles) and 16 h (open squares). Cell viability was determined using MTT and normalized to control (untreated) cells. Shown are mean ± SEM, n = 3. **b** HepaRG cells accumulate Mn with increasing Mn concentration. Cells were exposed to 50, 100, and 500 μM Mn for 4 or 16 h. Cells were washed with cold PBS, removed from the wells by trypsinization, and digested for ICP-MS analysis. Mn levels increased in the cells with increasing dose at

both the 4 and 16 h incubation periods. Values are mean ± SEM, n = 3 biological samples. *a*, significant from 50 μM; *b*, significant from 100 μM. **c** Shown is a diagram depicting the protocol used for the experimental results shown in C. HepaRG cells were pre-incubated with MnCl<sub>2</sub> for 4 or 16 h prior to the <sup>54</sup>Mn uptake assay. HepaRG cells were then rinsed and incubated with 1 μM <sup>54</sup>MnCl<sub>2</sub> for 30 min at 37 °C. Cells were rinsed, removed from the plate, and cell <sup>54</sup>Mn content determined using a gamma counter. **d** Values for the <sup>54</sup>Mn uptake experiment are shown as mean ± SEM, n = 4 biological; *a* significant from control; *b* significant from 5 μM, *c* significant from 50 μM. *P* < 0.05

accumulate in HepaRG cells in a dose-dependent manner over this concentration range and after these incubation periods (Fig. 2b). Mn accumulation by HepaRG cells was comparable to that measured in WIF-B cells exposed in a similar manner (Thompson et al. 2018).

Mn exposure decreases <sup>54</sup>Mn uptake by HepaRG cells

While ICP-MS can assess the mass accrual of metal, it does not report information about how uptake may be changing over time. Therefore, we also examined

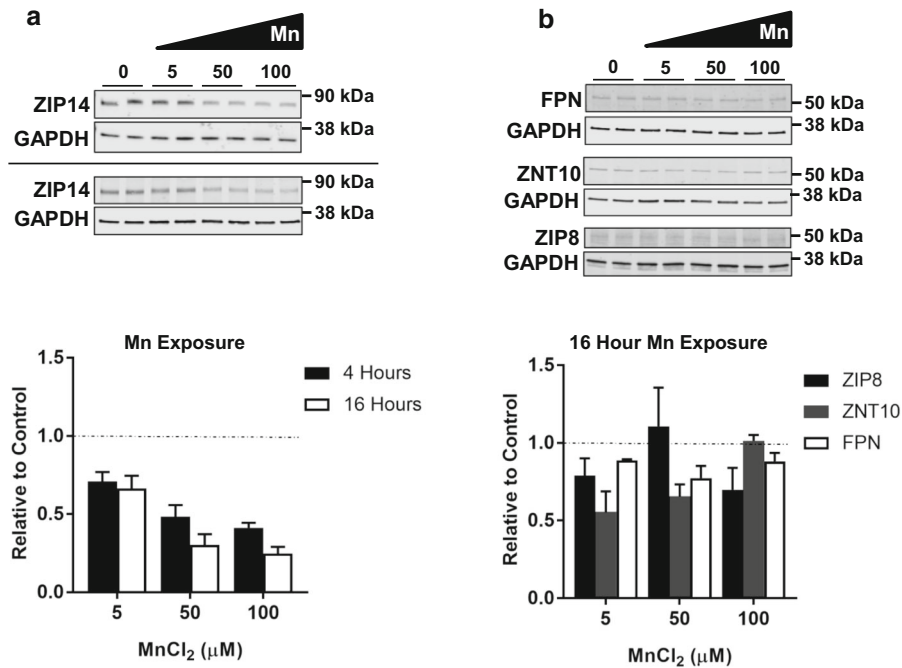


**Fig. 3** ZIP14 protein levels decrease in response to 4 and 16 h Mn exposure. HepaRG cells were treated with metal for 4 or 16 h in standard culture conditions. **a** Shown are representative Western blots for ZIP14 after 4 (top panel) and 16 h (bottom panel) treatment with MnCl<sub>2</sub>. Equal volumes of lysed samples were loaded per lane. ZIP14 band intensities were measured and normalized to GAPDH levels. Graphed are the normalized data at 5, 50, and 100 μM Mn where the control is set to 1 (dashed line). Values are mean ± SEM, n = 4 biological samples. ZIP14 protein levels in response to Mn exposure show a dose-

dependent regression at  $P < 0.05$ . **b** Shown are representative Western blots for FPN, ZNT10, and ZIP8 after 16 h treatment with MnCl<sub>2</sub>. Cell lysates were prepared for immunoblotting and equal volumes of lysed samples were loaded per lane. FPN, ZNT10, and ZIP8 band values were each normalized to GAPDH levels. Graphed are the normalized data at 5, 50, and 100 μM Mn. The control is set to 1 (dashed line). Values are mean ± SEM, n = 4 biological samples. ZIP8, ZntT10, and FPN do not show a dose-dependent regression

uptake dynamics in HepaRG cells following metal exposure for 4 or 16 h under standard culture conditions (see protocol design, Fig. 2c). Cells were subsequently incubated with a trace amount of <sup>54</sup>Mn to measure uptake. Up to 40% reduction in <sup>54</sup>Mn uptake was observed after incubation of HepaRG cells with Mn concentrations of 50 μM after the 4 h incubation period; import of the radiotracer was similarly reduced after the longer 16 h exposure time (Fig. 2d). Although Mn uptake was not completely suppressed, these results suggest that HepaRG cells respond to Mn exposure by down-regulating transport of the metal.

#### Mn exposure decreases ZIP14 protein levels

We postulated that one-way HepaRG cells could decrease Mn uptake following metal exposure was by down-regulating ZIP14. We therefore examined protein levels of ZIP14 by Western analysis of HepaRG

cell lysates collected after exposure to Mn. Treatment of HepaRG cells with MnCl<sub>2</sub> (5, 50, or 100 μM) for 4 and 16 h in standard culture conditions resulted in a dose-dependent decrease in ZIP14 protein levels (Fig. 3a). Similar results were found for cells treated with Mn for 16 h. Levels of HepaRG cell ZIP14 did not decrease when exposed to ZnSO<sub>4</sub> at equivalent concentrations over the same period of time, indicating this effect was specific to MnCl<sub>2</sub> exposure (data not shown). In contrast, levels of other transporters, including FPN, ZNT10 and ZIP8, did not decrease in a dose dependent manner (Fig. 3b).

#### Bafilomycin A1 blocks Mn-induced degradation of ZIP14

To examine the pathway of ZIP14 down-regulation in response to Mn, HepaRG cells were treated with bafilomycin A1, an inhibitor of vacuolar ATPases.

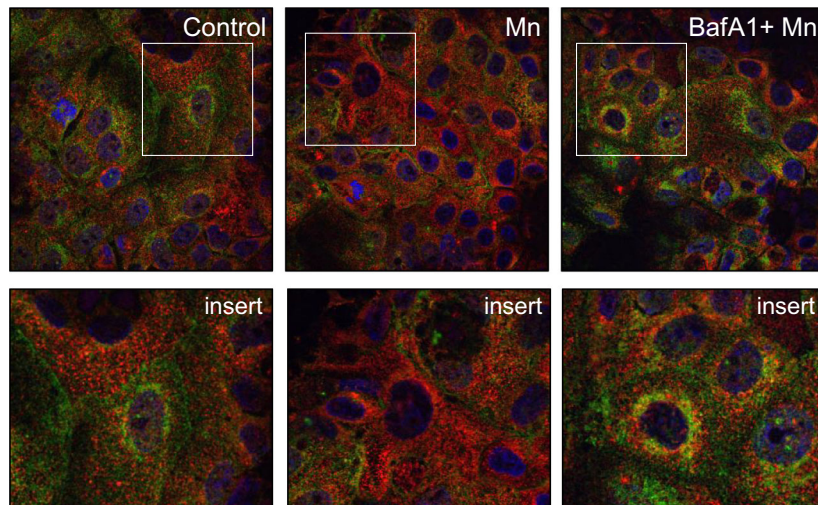
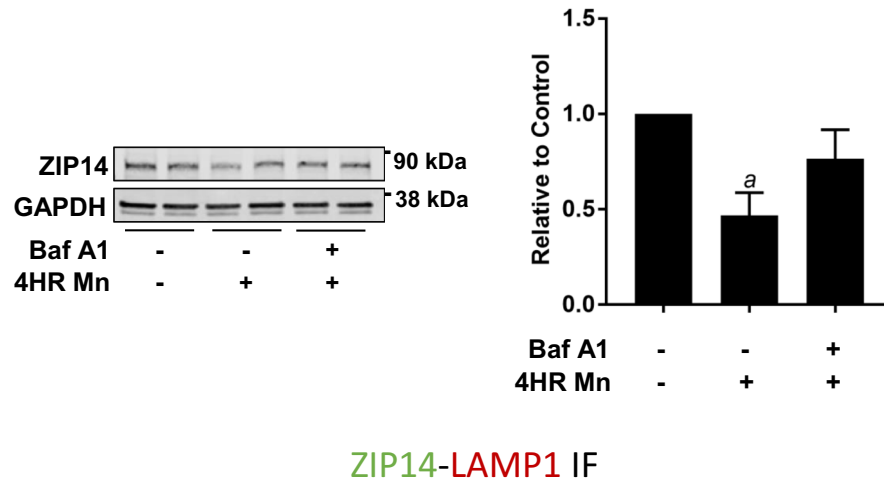


**Fig. 4** Bafilomycin A1 prevents Mn directed ZIP14 degradation. HepaRG cells were pretreated with 50 nM bafilomycin A1 (Baf A1) for 30 min prior to and during incubation with 50  $\mu$ M Mn for 4 additional hours. *Top panel*: Western analysis indicates ZIP14 levels are similar to control with Baf A1 treatment. Shown is a representative blot. Equal volumes of lysed samples were loaded per lane. ZIP14 band intensity was measured and normalized to GAPDH levels. Values are mean  $\pm$  SEM,  $n = 4$ ; *a* significant from control.  $P < 0.05$ . *Bottom panel*: Shown are representative staining examples for ZIP14 (green) and Lamp1 (red) in the same treatment groups using indirect

immunofluorescence. Below each image is an insert from the region indicated (white inset). IF experiments were performed in triplicate on two separate occasions. Image analysis was performed using ImageJ software and the JaCoP plugin to determine the Pearson's coefficients expressed as mean  $\pm$  SD: Control =  $0.275 \pm 0.020$ , Mn =  $0.234 \pm 0.018$ , and BafA1 + Mn =  $0.364 \pm 0.039$ . Pearson values for Bafilomycin A1-treated cells were significantly different from HepaRG cells in control conditions ( $P = 0.0004$ ) and Mn-treated cells ( $P < 0.0001$ ). Mn-treated cells were significantly different from control ( $P = 0.0045$ )

Bafilomycin A1 inhibits degradation in the endolysosomal pathway by raising vesicular pH to interfere with lysosomal protease activity. Western blot analysis of cell lysates from untreated control and Mn-treated samples indicated that the presence of bafilomycin A1 prevented the loss of ZIP14 (Fig. 4, top panel). Indirect immunofluorescence microscopy confirmed that ZIP14

degradation was blocked and further showed that bafilomycin A1 increased overlap between Lamp1-positive and ZIP14-positive structures in HepaRG cells (Fig. 4, bottom panel, BafA1 + Mn). Pearson values were  $0.275 \pm 0.020$  for control, Mn =  $0.234 \pm 0.018$  for Mn-treated, and  $0.364 \pm 0.039$  for bafilomycin A1-treated cells. Values are mean  $\pm$  SD. These results



support the idea that Mn induces ZIP14 down-regulation by redirecting the protein to the lysosomal pathway and that bafilomycin A1 arrests down-regulation by blocking transporter degradation.

### Effects of Mn on cellular stress

Mn exposure has been shown to alter the Golgi and Golgi-associated proteins including TMEM165, a trans-membrane Golgi protein thought to be involved in glycosylation (Dulary et al. 2017; Foulquier et al. 2012; Potelle et al. 2017; Rosnoblet et al. 2013a, b), and the Mn sensor GPP130, a receptor for Shiga toxin (Mukhopadhyay et al. 2010, 2013; Mukhopadhyay and Linstedt 2011). To compare the response of HepaRG cell Golgi proteins and other stress markers, Western blot analysis was carried out after exposure to 5, 50 or 100  $\mu\text{M}$   $\text{MnCl}_2$ . TMEM165 was reduced by  $\sim 60\%$  after 4 h of exposure at the lowest concentration studied (Fig. 5, left panel); no further reduction was observed at 16 h (data not shown). In contrast, protein levels of GPP130 and the *cis*-Golgi marker GM130 were unaffected after 4 h of incubation (Fig. 5, left panel). However, longer periods of Mn exposure (16 h) did induce the ER stress marker BiP and decreased GPP130 levels (Fig. 5, right panel) as previously reported (Mukhopadhyay et al. 2010; Potelle et al. 2017). The control *cis*-Golgi marker GM130 remained unchanged under both conditions (Fig. 5). These combined results indicate that exposure of HepaRG cells to Mn induces organellar stress affecting the secretory pathway with selective loss of Mn regulated membrane proteins.

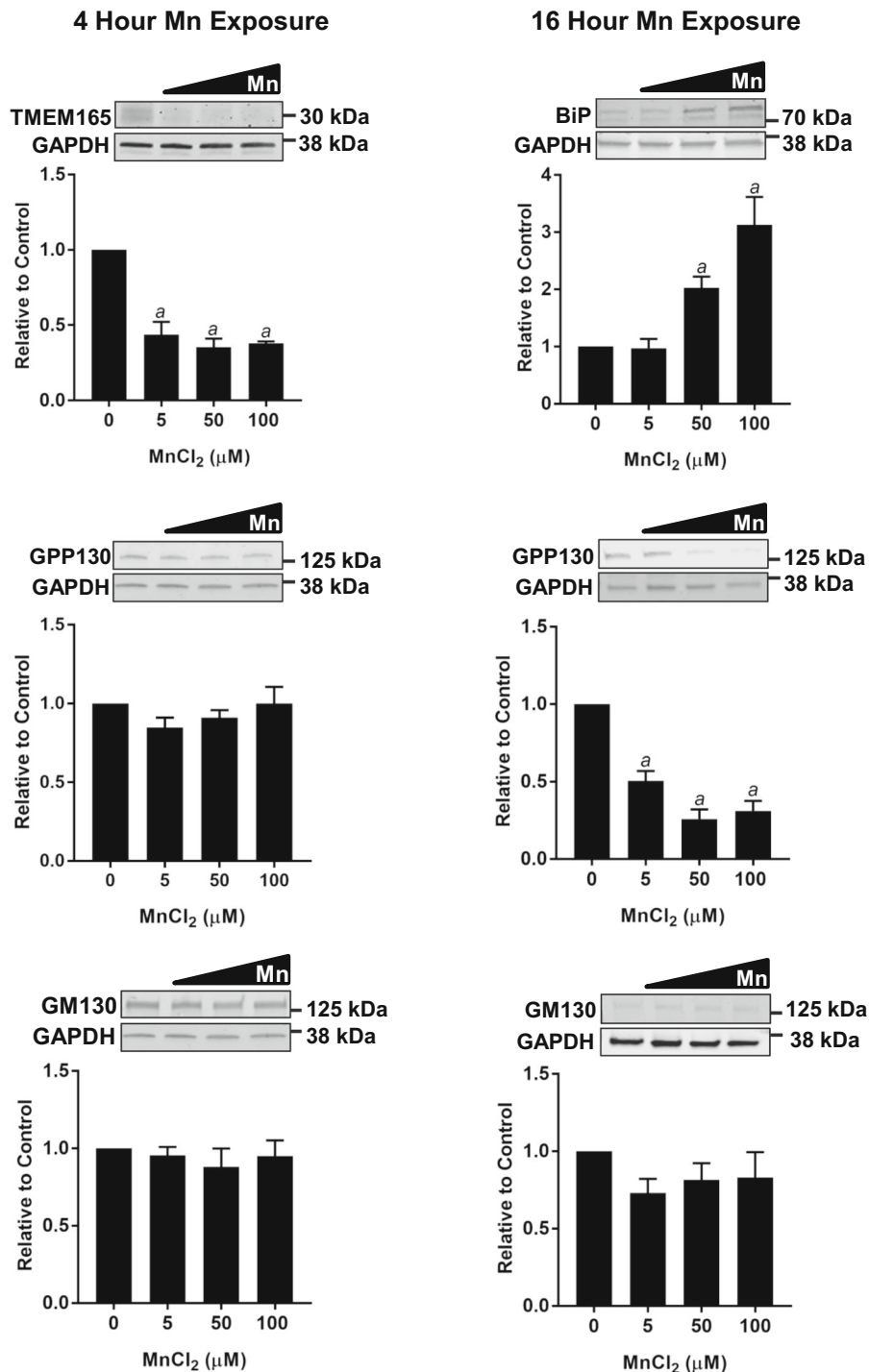
### Discussion

Mn homeostasis is necessary to handle this essential yet toxic mineral. Elimination of excess circulating Mn is critical to protect the brain and central nervous system. Environmental and occupational exposure to Mn can lead to the metal's deposition in the basal ganglia and subthalamic regions causing disruption of motor and cognitive pathways known as manganism (Kwakye et al. 2015). Interestingly Mn also accumulates in these areas during cholestasis and hepatobiliary dysfunction (Ikeda et al. 2000a, b; Rose et al. 1999). A prevalent view is that the liver is the organ responsible for the clearance of ingested Mn through

the first-pass-hepatic clearance system, although increasing evidence supports a crucial role for the intestine in the regulation of circulating levels (Scheiber et al. 2019; Taylor et al. 2019). A number of recent genetic studies have determined that disruptions in Mn acquisition, accumulation and deposition result from defects in human genes thought to be involved in Mn transport and homeostasis, including *SLC39A14* (ZIP14), *SLC39A8* (ZIP8), and *SLC30A10* (ZNT10) (Aydemir et al. 2017; Boycott et al. 2015; Choi et al. 2019; Hutchens et al. 2017; Jenkitkasemwong et al. 2018; Lin et al. 2017; Liu et al. 2017; Marti-Sanchez et al. 2018; Park et al. 2015; Quadri et al. 2012, 2015; Riley et al. 2017; Xin et al. 2017). In particular, human mutations in ZIP14 lead to hypermanganesemia and neurological disorders.

ZIP14 is a transmembrane protein consisting of 8 transmembrane domains with an intramembrane metal-binding site that forms a pore for metal transport (Aydemir and Cousins 2018; Eide 2006; Kambe et al. 2015; Taylor et al. 2005). The protein is thought to function as a dimer or multimer in the formation of ion channels for metal transport (Heitzer and Hallmann 2002; Lichten and Cousins 2009). ZIP14 is a member of the SLC39A family of transporters primarily identified as zinc transporters. Studies in murine hepatocytes found that an increase in ZIP14 expression was coupled with an increase in cellular zinc accumulation (Lichten and Cousins 2009). It is known to play a role in iron uptake and clearance by the liver (Gao et al. 2008; Jenkitkasemwong et al. 2018; Liuzzi et al. 2006; Zhao et al. 2010). While zinc and iron are substrates for transport, ZIP14 is also thought to be the primary transporter involved in Mn uptake (Aydemir and Cousins 2018; Girijashanker et al. 2008; Pinilla-Tenas et al. 2011). ZIP14 knockout mice display reduced liver Mn levels with elevated concentrations in blood and other systemic organs giving further evidence of its role in Mn import (Aydemir et al. 2017; Jenkitkasemwong et al. 2018; Xin et al. 2017).

To study Mn uptake and ZIP14 function in hepatocytes, we employed HepaRG cells which are able to polarize and express markers for both basolateral and apical membranes, providing a useful alternative to human primary hepatocytes (Antherieu et al. 2013; Bachour-El Azzi et al. 2015; Kanebratt and Andersson 2008; Sharanek et al. 2014). Our results confirm the expression of ZIP14 and its localization at the HepaRG cell basolateral surface, a distribution that



would facilitate the movement of Mn into these hepatocytes. This result is consistent with previous reports localizing ZIP14 to the basolateral membrane

of enterocytes (Guthrie et al. 2015) and WIF-B hepatocytes (Thompson et al. 2018). <sup>54</sup>Mn uptake studies revealed HepaRG cells accumulate Mn in a

◀ **Fig. 5** Golgi markers are altered by 4 h Mn exposure (left panel). HepaRG cells were treated with Mn for 4 h at the indicated concentrations in standard culture conditions. Shown are the results of Western analysis. Cell lysates were prepared for immunoblotting and equal volumes of lysed samples were loaded per lane. TMEM165, GPP130, and GM130 band intensities each were measured and normalized to GAPDH levels. The transmembrane Golgi protein TMEM165 decreased during acute 4 h Mn exposure without any change in the Mn sensor GPP130 or *cis*-Golgi marker GM130. Values are mean  $\pm$  SEM,  $n = 4$  biological samples; *a* significant from control.  $P < 0.05$ . Prolonged 16 h Mn exposure exacerbates Golgi and ER stress (right panel). HepaRG cells were treated with Mn for 16 h at the indicated concentrations in standard culture conditions. Shown are representative blots and the results of Western analysis (graphs). Cell lysates were prepared for immunoblotting and equal volumes of lysed samples were loaded per lane. BiP, GPP130, and GM130 band intensities each were measured and normalized to GAPDH levels. The ER stress response protein BiP increased with prolonged Mn exposure. The Mn sensor GPP130 decreased as an indication of increased Golgi stress. The *cis*-Golgi marker GM130 remained unchanged. TMEM165 was decreased similarly to 4 h exposure (data not shown). Values are mean  $\pm$  SEM,  $n = 4$  biological samples; *a* significant from control.  $P < 0.05$

time- and temperature-dependent manner and that uptake was competed by excess Mn.

Despite robust Mn uptake, we observed that HepaRG cells remained viable even after 16 h of exposure of up to 1000  $\mu$ M Mn. In contrast, WIF-B hepatocytes have decreased viability after 16 h of exposure to 500  $\mu$ M Mn (Leitch et al. 2011; Thompson et al. 2018). ICP-MS experiments confirmed the dose-dependent accumulation of the metal by HepaRG cells under these conditions. However, we also observed that uptake of  $^{54}$ Mn was diminished upon pre-exposure to the metal, suggesting that one way these cells preserve their integrity is to reduce uptake of the metal. This idea is supported by the fact that ZIP14 protein levels are decreased by exposure to Mn in a dose-dependent manner. This effect appears to be a specific response to Mn since exposure to Zn did not alter ZIP14 levels (data not shown). Moreover, protein levels of other known Mn transporters detected in HepaRG cells (ZIP8, ZNT10, or FPN) did not change in a dose-dependent manner. Previous studies have shown that the iron regulator HFE decreases ZIP14 stability in HepG2 hepatocytes (Gao et al. 2008) and that iron exposure induces degradation by the proteosomal pathway (Zhao et al. 2014). Thus, the regulation of ZIP14 appears to respond to selective

metal substrates that direct the protein to specific degradatory pathways (lysosomal versus proteosomal).

In contrast to human HepaRG cells, levels of ZIP14 in WIF-B cells did not change upon incubation with up to 500  $\mu$ M MnCl<sub>2</sub> (Thompson et al. 2018). We do not know if uptake is affected by pre-exposure to Mn. However, WIF-B cells are a rat/human hybrid line and we determined that both rat and human ZIP14 were expressed by these hepatocytes. As noted above, the WIF-B cells do not display the same resistance to Mn cytotoxicity observed in the HepaRG cell experiments we report here, possibly due to the hybrid nature of hepatic components. The lack of ZIP14 down-regulation in WIF-B cells is most likely one factor contributing to their Mn sensitivity. The failure of WIF-B cells to down-regulate ZIP14 is possibly an effect of co-expression of both transporters without the companion trafficking machinery to enable a reduction of its function.

Can down-regulation of ZIP14 maintain hepatocyte viability while preventing Mn accumulation in extrahepatic tissues? Studies by Xin et al. (2017) using *Slc39a14<sup>fl/fl</sup>; Alb-Cre+* liver specific ZIP14 knockout mice showed that these mice do not accumulate Mn in the brain or other extrahepatic tissues and do not develop motor deficits. This result indicates that the selective loss of *Slc39a14* expression in hepatocytes is not sufficient to cause Mn accumulation. A more recent study by Scheiber et al. (2019) found ZIP14 present on the basolateral membrane of enterocytes. Their studies in CaCo-2 ZIP14 knockout cells and intestine-specific ZIP14 knockout mice revealed ZIP14 restricts dietary Mn absorption. This additional Mn regulatory feedback mechanism might respond to liver-specific changes in ZIP14. To confirm our observations in HepaRG cells, it would be interesting to investigate levels of ZIP14 in *Slc30a10* knockout mice which have high hepatic Mn (Hutchens et al. 2017).

One caveat to our study are the supraphysiologic levels of Mn observed to alter uptake and ZIP14 levels. It should be noted that serum proteins that can bind divalent cations (albumin, alpha2-macroglobulin) are present in the culture medium thus reducing the concentration of actual free metal available for cell uptake. Studies of Mn toxicity and cytotoxicity typically use  $\mu$ M concentrations for extended exposure periods (Girijashanker et al. 2008; Pinilla-Tenas

et al. 2011). Bowman and Aschner (2014) have estimated neurotoxicity occurs at intracellular levels of 60–160  $\mu\text{M}$  Mn in the brain (Bowman and Aschner 2014).

The Golgi apparatus appears to play an important role in cellular Mn homeostasis and effects on its function often occur over the Mn concentration range used for our studies (Carmona et al. 2019; Houdou et al. 2019). In fact, previous studies examining Mn-regulated proteins included treatments of cells with 1–500  $\mu\text{M}$  Mn over time courses ranging from 1 to 24 h (Masuda et al. 2013; Mukhopadhyay et al. 2010; Potelle et al. 2017; Tewari et al. 2015; Towler et al. 2000). For example, treatment of cells with 500  $\mu\text{M}$   $\text{MnCl}_2$  induces rapid redistribution and lysosomal degradation of the Mn sensor protein GPP130 (Mukhopadhyay et al. 2010). In addition, the Golgi protein TMEM165 is down-regulated in response to Mn exposure and chloroquine has been shown to block Mn-induced lysosomal degradation of this protein (Potelle et al. 2017). We observed that Mn-induced degradation of ZIP14 by HepaRG cells is blocked by bafilomycin A1, indicating the transporter is similarly trafficked towards the lysosome for its down-regulation in the presence of the metal. The observation that ZIP14 localizes to Lamp1-positive vesicles in bafilomycin A1-treated HepaRG cells in the presence of Mn confirms the HepaRG cell trafficking response. The fast degradation response of TMEM165 and delayed GPP130 response observed for HepaRG cells upon Mn exposure is consistent with previous studies (Potelle et al. 2017). These differences may reflect that Mn is “sensed” by the cytoplasmic domain of TMEM165 (Potelle et al. 2017) but the luminal domain of GPP130 (Mukhopadhyay et al. 2010) such that time necessary for Mn uptake by the Golgi is reflected by the latter time course for degradation. We do not yet know the structural elements involved in Zip14 degradation.

Mn is required for several cellular processes, including membrane protein glycosylation. TMEM165, a transmembrane Golgi protein, is thought to be involved in glycosylation reactions and has been found to decrease in response to  $\mu\text{M}$  levels of Mn. Similarly, the Mn sensing protein GPP130 was found to decrease with high levels of Mn. Our study also found TMEM165 and GPP130 were affected by high Mn levels in hepatocytes and correlated with decreased ZIP14. Loss of ZIP14 may possibly help

to decrease Mn entry into the cell and its accumulation in the Golgi. Many studies suggest that intracellular toxic levels of Mn can be sensed by the Golgi and can initiate cellular stress responses to prevent cell death. We do not yet know how ZIP14 may be regulated by cellular Mn levels but its regulation may reflect a hepatocyte-specific global response to Mn detoxification. It should be noted that the longer 16 h Mn exposure also induced BiP, an indicator of ER stress. This observation is also consistent with studies in other cells types demonstrating that exposure to Mn can induce ER stress and cell death (Chun et al. 2001; Mahadevan et al. 2012; Wang et al. 2015; Wu et al. 2019; Yoon et al. 2011). Ultimately, the down-regulation of ZIP14 could provide a cytoprotective response to maintain cell viability.

**Acknowledgements** This work was supported by a grant from the US National Institutes of Health, National Institute of Environmental Health Sciences (R56 ES0146380). ICP-MS work was supported by the Trace Element Shared Resource, NCI Cancer Center Support Grant 5P30CA023108-37, NIEHS Superfund Grant P42 ES007373.

**Open Access** This article is distributed under the terms of the Creative Commons Attribution 4.0 International License (<http://creativecommons.org/licenses/by/4.0/>), which permits unrestricted use, distribution, and reproduction in any medium, provided you give appropriate credit to the original author(s) and the source, provide a link to the Creative Commons license, and indicate if changes were made.

## References

- Aninat C, Piton A, Glaise D et al (2006) Expression of cytochromes P450, conjugating enzymes and nuclear receptors in human hepatoma HepaRG cells. *Drug Metab Dispos* 34(1):75–83. <https://doi.org/10.1124/dmd.105.006759>
- Antherieu S, Bachour-El Azzi P, Dumont J et al (2013) Oxidative stress plays a major role in chlorpromazine-induced cholestasis in human HepaRG cells. *Hepatology* 57(4):1518–1529. <https://doi.org/10.1002/hep.26160>
- Aschner JL, Aschner M (2005) Nutritional aspects of manganese homeostasis. *Mol Aspects Med* 26(4–5):353–362. <https://doi.org/10.1016/j.mam.2005.07.003>
- Aschner M, Erikson K (2017) Manganese. *Adv Nutr* 8(3):520–521. <https://doi.org/10.3945/an.117.015305>
- Aydemir TB, Cousins RJ (2018) The multiple faces of the metal transporter ZIP14 (SLC39A14). *J Nutr* 148(2):174–184. <https://doi.org/10.1093/jn/nxx041>
- Aydemir TB, Kim MH, Kim J et al (2017) Metal transporter Zip14 (Slc39a14) deletion in mice increases manganese deposition and produces neurotoxic signatures and

- diminished motor activity. *J Neurosci* 37(25):5996–6006. <https://doi.org/10.1523/JNEUROSCI.0285-17.2017>
- Bachour-El Azzi P, Sharanek A, Burbán A et al (2015) Comparative localization and functional activity of the main hepatobiliary transporters in HepaRG cells and primary human hepatocytes. *Toxicol Sci* 145(1):157–168. <https://doi.org/10.1093/toxsci/kfv041>
- Bowers K, Srai SKS (2018) The trafficking of metal ion transporters of the Zrt- and Irt-like protein family. *Traffic* 19(11):813–822. <https://doi.org/10.1111/tra.12602>
- Bowman AB, Aschner M (2014) Considerations on manganese (Mn) treatments for in vitro studies. *Neurotoxicology* 41:141–142. <https://doi.org/10.1016/j.neuro.2014.01.010>
- Boycott KM, Beaulieu CL, Kernohan KD et al (2015) Autosomal-recessive intellectual disability with cerebellar atrophy syndrome caused by mutation of the manganese and zinc transporter gene SLC39A8. *Am J Hum Genet* 97(6):886–893. <https://doi.org/10.1016/j.ajhg.2015.11.002>
- Carmona A, Zogzas CE, Roudeau S et al (2019) SLC30A10 mutation involved in parkinsonism results in manganese accumulation within nanovesicles of the Golgi apparatus. *ACS Chem Neurosci* 10(1):599–609. <https://doi.org/10.1021/acchemneuro.8b00451>
- Choi EK, Nguyen TT, Iwase S, Seo YA (2019) Ferroportin disease mutations influence manganese accumulation and cytotoxicity. *FASEB J* 33(2):2228–2240. <https://doi.org/10.1096/fj.201800831R>
- Chun HS, Lee H, Son JH (2001) Manganese induces endoplasmic reticulum (ER) stress and activates multiple caspases in nigral dopaminergic neuronal cells, SN4741. *Neurosci Lett* 316(1):5–8
- Clayton PT (2017) Inherited disorders of transition metal metabolism: an update. *J Inher Metab Dis* 40(4):519–529. <https://doi.org/10.1007/s10545-017-0030-x>
- Crinella FM (2012) Does soy-based infant formula cause ADHD? Update and public policy considerations. *Expert Rev Neurother* 12(4):395–407. <https://doi.org/10.1586/ern.12.2>
- Dulary E, Potelle S, Legrand D, Foulquier F (2017) TMEM165 deficiencies in congenital disorders of glycosylation type II (CDG-II): clues and evidences for roles of the protein in Golgi functions and ion homeostasis. *Tissue Cell* 49(2 Pt A):150–156. <https://doi.org/10.1016/j.tice.2016.06.006>
- Eide DJ (2006) Zinc transporters and the cellular trafficking of zinc. *Biochim Biophys Acta* 1763(7):711–722. <https://doi.org/10.1016/j.bbamcr.2006.03.005>
- Fernandes J, Chandler JD, Liu KH et al (2019) Metabolomic responses to manganese dose in SH-SY5Y human neuroblastoma cells. *Toxicol Sci* 169(1):84–94. <https://doi.org/10.1093/toxsci/kfz028>
- Foulquier F, Amyere M, Jaeken J et al (2012) TMEM165 deficiency causes a congenital disorder of glycosylation. *Am J Hum Genet* 91(1):15–26. <https://doi.org/10.1016/j.ajhg.2012.05.002>
- Gao J, Zhao N, Knutson MD, Enns CA (2008) The hereditary hemochromatosis protein, HFE, inhibits iron uptake via down-regulation of Zip14 in HepG2 cells. *J Biol Chem* 283(31):21462–21468. <https://doi.org/10.1074/jbc.M803150200>
- Girijashanker K, He L, Soleimani M et al (2008) Slc39a14 gene encodes ZIP14, a metal/bicarbonate symporter: similarities to the ZIP8 transporter. *Mol Pharmacol* 73(5):1413–1423. <https://doi.org/10.1124/mol.107.043588>
- Guthrie GJ, Aydemir TB, Troche C, Martin AB, Chang SM, Cousins RJ (2015) Influence of ZIP14 (slc39A14) on intestinal zinc processing and barrier function. *Am J Physiol Gastrointest Liver Physiol* 308(3):G171–G178. <https://doi.org/10.1152/ajpgi.00021.2014>
- Heitzer M, Hallmann A (2002) An extracellular matrix-localized metalloproteinase with an exceptional QEXXH metal binding site prefers copper for catalytic activity. *J Biol Chem* 277(31):28280–28286. <https://doi.org/10.1074/jbc.M203925200>
- Hong JS, Hung CR, Seth PK, Mason G, Bondy SC (1984) Effect of manganese treatment on the levels of neurotransmitters, hormones, and neuropeptides: modulation by stress. *Environ Res* 34(2):242–249
- Houdou M, Lebredonchel E, Garat A et al (2019) Involvement of thapsigargin- and cyclopiazonic acid-sensitive pumps in the rescue of TMEM165-associated glycosylation defects by Mn(2). *FASEB J* 33(2):2669–2679. <https://doi.org/10.1096/fj.201800387R>
- Hutchens S, Liu C, Jursa T et al (2017) Deficiency in the manganese efflux transporter SLC30A10 induces severe hypothyroidism in mice. *J Biol Chem* 292(23):9760–9773. <https://doi.org/10.1074/jbc.M117.783605>
- Ikeda S, Sera Y, Yoshida M et al (2000a) Manganese deposits in patients with biliary atresia after hepatic porto-enterostomy. *J Pediatr Surg* 35(3):450–453
- Ikeda S, Yamaguchi Y, Sera Y et al (2000b) Manganese deposition in the globus pallidus in patients with biliary atresia. *Transplantation* 69(11):2339–2343
- Jenkitkasemwong S, Akinyode A, Paulus E et al (2018) SLC39A14 deficiency alters manganese homeostasis and excretion resulting in brain manganese accumulation and motor deficits in mice. *Proc Natl Acad Sci USA* 115(8):E1769–E1778. <https://doi.org/10.1073/pnas.1720739115>
- Juneja M, Shamim U, Joshi A et al (2018) A novel mutation in SLC39A14 causing hypermanganesemia associated with infantile onset dystonia. *J Gene Med* 20(4):e3012. <https://doi.org/10.1002/jgm.3012>
- Kambe T, Tsuji T, Hashimoto A, Itsumura N (2015) The physiological, biochemical, and molecular roles of zinc transporters in zinc homeostasis and metabolism. *Physiol Rev* 95(3):749–784. <https://doi.org/10.1152/physrev.00035.2014>
- Kanebratt KP, Andersson TB (2008) Evaluation of HepaRG cells as an in vitro model for human drug metabolism studies. *Drug Metab Dispos* 36(7):1444–1452. <https://doi.org/10.1124/dmd.107.020016>
- Kwakyé GF, Paoliello MM, Mukhopadhyay S, Bowman AB, Aschner M (2015) Manganese-induced parkinsonism and parkinson's disease: shared and distinguishable features. *Int J Environ Res Public Health* 12(7):7519–7540. <https://doi.org/10.3390/ijerph120707519>
- Le Vee M, Jigorel E, Glaise D, Gripon P, Guguen-Guillouzo C, Fardel O (2006) Functional expression of sinusoidal and canalicular hepatic drug transporters in the differentiated human hepatoma HepaRG cell line. *Eur J Pharm Sci* 28(1–2):109–117. <https://doi.org/10.1016/j.ejps.2006.01.004>

- Leitch S, Feng M, Muend S, Braiterman LT, Hubbard AL, Rao R (2011) Vesicular distribution of secretory pathway  $\text{Ca}^{2+}$ -ATPase isoform 1 and a role in manganese detoxification in liver-derived polarized cells. *Biometals* 24(1):159–170. <https://doi.org/10.1007/s10534-010-9384-3>
- Lichten LA, Cousins RJ (2009) Mammalian zinc transporters: nutritional and physiologic regulation. *Annu Rev Nutr* 29:153–176. <https://doi.org/10.1146/annurev-nutr-033009-083312>
- Lin W, Vann DR, Doulias PT et al (2017) Hepatic metal ion transporter ZIP8 regulates manganese homeostasis and manganese-dependent enzyme activity. *J Clin Invest* 127(6):2407–2417. <https://doi.org/10.1172/JCI90896>
- Liu C, Hutchens S, Jursa T et al (2017) Hypothyroidism induced by loss of the manganese efflux transporter SLC30A10 may be explained by reduced thyroxine production. *J Biol Chem* 292(40):16605–16615. <https://doi.org/10.1074/jbc.M117.804989>
- Liuzzi JP, Aydemir F, Nam H, Knutson MD, Cousins RJ (2006) Zip14 (Slc39a14) mediates non-transferrin-bound iron uptake into cells. *Proc Natl Acad Sci USA* 103(37):13612–13617. <https://doi.org/10.1073/pnas.0606424103>
- Lucchini R, Bergamaschi E, Smargiassi A, Festa D, Apostoli P (1997) Motor function, olfactory threshold, and hematological indices in manganese-exposed ferroalloy workers. *Environ Res* 73(1–2):175–180. <https://doi.org/10.1006/enrs.1997.3702>
- Mahadevan NR, Anufreichick V, Rodvold JJ, Chiu KT, Sepulveda H, Zanetti M (2012) Cell-extrinsic effects of tumor ER stress imprint myeloid dendritic cells and impair CD8(+) T cell priming. *PLoS ONE* 7(12):e51845. <https://doi.org/10.1371/journal.pone.0051845>
- Marti-Sanchez L, Ortigoza-Escobar JD, Darling A et al (2018) Hypermanganesemia due to mutations in SLC39A14: further insights into Mn deposition in the central nervous system. *Orphanet J Rare Dis* 13(1):28. <https://doi.org/10.1186/s13023-018-0758-x>
- Masuda M, Braun-Sommargren M, Crooks D, Smith DR (2013) Golgi phosphoprotein 4 (GPP130) is a sensitive and selective cellular target of manganese exposure. *Synapse* 67(5):205–215. <https://doi.org/10.1002/syn.21632>
- Mukhopadhyay S, Linstedt AD (2011) Identification of a gain-of-function mutation in a Golgi P-type ATPase that enhances  $\text{Mn}^{2+}$  efflux and protects against toxicity. *Proc Natl Acad Sci USA* 108(2):858–863. <https://doi.org/10.1073/pnas.1013642108>
- Mukhopadhyay S, Bachert C, Smith DR, Linstedt AD (2010) Manganese-induced trafficking and turnover of the *cis*-Golgi glycoprotein GPP130. *Mol Biol Cell* 21(7):1282–1292. <https://doi.org/10.1091/mbc.E09-11-0985>
- Mukhopadhyay S, Redler B, Linstedt AD (2013) Shiga toxin-binding site for host cell receptor GPP130 reveals unexpected divergence in toxin-trafficking mechanisms. *Mol Biol Cell* 24(15):2311–2318. <https://doi.org/10.1091/mbc.E13-01-0057>
- Park JH, Hogrebe M, Gruneberg M et al (2015) SLC39A8 deficiency: a disorder of manganese transport and glycosylation. *Am J Hum Genet* 97(6):894–903. <https://doi.org/10.1016/j.ajhg.2015.11.003>
- Pernelle K, Le Guevel R, Glaise D et al (2011) Automated detection of hepatotoxic compounds in human hepatocytes using HepaRG cells and image-based analysis of mitochondrial dysfunction with JC-1 dye. *Toxicol Appl Pharmacol* 254(3):256–266. <https://doi.org/10.1016/j.taap.2011.04.018>
- Pihl RO, Parkes M (1977) Hair element content in learning disabled children. *Science* 198(4313):204–206
- Pinilla-Tenas JJ, Sparkman BK, Shawki A et al (2011) Zip14 is a complex broad-scope metal-ion transporter whose functional properties support roles in the cellular uptake of zinc and nontransferrin-bound iron. *Am J Physiol Cell Physiol* 301(4):C862–C871. <https://doi.org/10.1152/ajpcell.00479.2010>
- Porte Alcon S, Gorojod RM, Kotler ML (2018) Regulated necrosis orchestrates microglial cell death in manganese-induced toxicity. *Neuroscience* 393:206–225. <https://doi.org/10.1016/j.neuroscience.2018.10.006>
- Potelle S, Dulary E, Climer L et al (2017) Manganese-induced turnover of TMEM165. *Biochem J* 474(9):1481–1493. <https://doi.org/10.1042/BCJ20160910>
- Quadri M, Federico A, Zhao T et al (2012) Mutations in SLC30A10 cause parkinsonism and dystonia with hypermanganesemia, polycythemia, and chronic liver disease. *Am J Hum Genet* 90(3):467–477. <https://doi.org/10.1016/j.ajhg.2012.01.017>
- Quadri M, Kamate M, Sharma S et al (2015) Manganese transport disorder: novel SLC30A10 mutations and early phenotypes. *Mov Disord* 30(7):996–1001. <https://doi.org/10.1002/mds.26202>
- Riley LG, Cowley MJ, Gayevskiy V et al (2017) A SLC39A8 variant causes manganese deficiency, and glycosylation and mitochondrial disorders. *J Inher Metab Dis* 40(2):261–269. <https://doi.org/10.1007/s10545-016-0010-6>
- Rodan LH, Hauptman M, D’Gama AM et al (2018) Novel founder intronic variant in SLC39A14 in two families causing Manganism and potential treatment strategies. *Mol Genet Metab* 124(2):161–167. <https://doi.org/10.1016/j.ymgme.2018.04.002>
- Rose C, Butterworth RF, Zayed J et al (1999) Manganese deposition in basal ganglia structures results from both portal-systemic shunting and liver dysfunction. *Gastroenterology* 117(3):640–644
- Rosnoblet C, Legrand D, Demaegd D et al (2013a) Impact of disease-causing mutations on TMEM165 subcellular localization, a recently identified protein involved in CDG-II. *Hum Mol Genet* 22(14):2914–2928. <https://doi.org/10.1093/hmg/ddt146>
- Rosnoblet C, Peanne R, Legrand D, Foulquier F (2013b) Glycosylation disorders of membrane trafficking. *Glycoconj J* 30(1):23–31. <https://doi.org/10.1007/s10719-012-9389-y>
- Roth JA (2006) Homeostatic and toxic mechanisms regulating manganese uptake, retention, and elimination. *Biol Res* 39(1):45–57
- Roth JA, Horbinski C, Higgins D, Lein P, Garrick MD (2002) Mechanisms of manganese-induced rat pheochromocytoma (PC12) cell death and cell differentiation. *Neurotoxicology* 23(2):147–157
- Scheiber IF, Wu Y, Morgan SE, Zhao N (2019) The intestinal metal transporter ZIP14 maintains systemic manganese

- homeostasis. *J Biol Chem.* <https://doi.org/10.1074/jbc.RA119.008762>
- Sharanek A, Azzi PB, Al-Attrache H et al (2014) Different dose-dependent mechanisms are involved in early cyclosporine a-induced cholestatic effects in hepaRG cells. *Toxicol Sci* 141(1):244–253. <https://doi.org/10.1093/toxsci/kfu122>
- Suda J, Zhu L, Karvar S (2011) Phosphorylation of radixin regulates cell polarity and Mrp-2 distribution in hepatocytes. *Am J Physiol Cell Physiol* 300(3):C416–C424. <https://doi.org/10.1152/ajpcell.00467.2010>
- Susukida T, Sekine S, Nozaki M et al (2016) Establishment of a drug-induced, bile acid-dependent hepatotoxicity model using HepaRG cells. *J Pharm Sci* 105(4):1550–1560. <https://doi.org/10.1016/j.xphs.2016.01.013>
- Taylor KM, Morgan HE, Johnson A, Nicholson RI (2005) Structure–function analysis of a novel member of the LIV-1 subfamily of zinc transporters, ZIP14. *FEBS Lett* 579(2):427–432. <https://doi.org/10.1016/j.febslet.2004.12.006>
- Taylor CA, Hutchens S, Liu C et al (2019) SLC30A10 transporter in the digestive system regulates brain manganese under basal conditions while brain SLC30A10 protects against neurotoxicity. *J Biol Chem* 294(6):1860–1876. <https://doi.org/10.1074/jbc.RA118.005628>
- Tewari R, Bachert C, Linstedt AD (2015) Induced oligomerization targets Golgi proteins for degradation in lysosomes. *Mol Biol Cell* 26(24):4427–4437. <https://doi.org/10.1091/mbc.E15-04-0207>
- Thompson KJ, Hein J, Baez A, Sosa JC, Wessling-Resnick M (2018) Manganese transport and toxicity in polarized WIF-B hepatocytes. *Am J Physiol Gastrointest Liver Physiol* 315(3):G351–G363. <https://doi.org/10.1152/ajpgi.00103.2018>
- Towler MC, Prescott AR, James J, Lucocq JM, Ponnambalam S (2000) The manganese cation disrupts membrane dynamics along the secretory pathway. *Exp Cell Res* 259(1):167–179. <https://doi.org/10.1006/excr.2000.4958>
- Tran TT, Chowanadisai W, Lonnerdal B et al (2002) Effects of neonatal dietary manganese exposure on brain dopamine levels and neurocognitive functions. *Neurotoxicology* 23(4–5):645–651
- Tuschl K, Meyer E, Valdivia LE et al (2016) Mutations in SLC39A14 disrupt manganese homeostasis and cause childhood-onset parkinsonism-dystonia. *Nat Commun* 7:11601. <https://doi.org/10.1038/ncomms11601>
- Wang T, Li X, Yang D et al (2015) ER stress and ER stress-mediated apoptosis are involved in manganese-induced neurotoxicity in the rat striatum in vivo. *Neurotoxicology* 48:109–119. <https://doi.org/10.1016/j.neuro.2015.02.007>
- Wu C, Yuan G, Mo R, Huang Y, Luo T, Wang J (2019) Effect of endoplasmic reticulum stress involved in manganese-induced neurotoxicity in rats. *Mol Med Rep* 19(6):5169–5176. <https://doi.org/10.3892/mmr.2019.10175>
- Xin Y, Gao H, Wang J et al (2017) Manganese transporter Slc39a14 deficiency revealed its key role in maintaining manganese homeostasis in mice. *Cell Discov* 3:17025. <https://doi.org/10.1038/celldisc.2017.25>
- Yamada M, Ohno S, Okayasu I et al (1986) Chronic manganese poisoning: a neuropathological study with determination of manganese distribution in the brain. *Acta Neuropathol* 70(3–4):273–278
- Yoon H, Kim DS, Lee GH, Kim KW, Kim HR, Chae HJ (2011) Apoptosis induced by manganese on neuronal SK-N-MC cell line: endoplasmic reticulum (ER) stress and mitochondria dysfunction. *Environ Health Toxicol* 26:e2011017. <https://doi.org/10.5620/eh.2011.26.e2011017>
- Zhao N, Gao J, Enns CA, Knutson MD (2010) ZRT/IRT-like protein 14 (ZIP14) promotes the cellular assimilation of iron from transferrin. *J Biol Chem* 285(42):32141–32150. <https://doi.org/10.1074/jbc.M110.143248>
- Zhao N, Zhang AS, Worthen C, Knutson MD, Enns CA (2014) An iron-regulated and glycosylation-dependent proteasomal degradation pathway for the plasma membrane metal transporter ZIP14. *Proc Natl Acad Sci USA* 111(25):9175–9180. <https://doi.org/10.1073/pnas.1405355111>

**Publisher's Note** Springer Nature remains neutral with regard to jurisdictional claims in published maps and institutional affiliations.